the nonpolar agents used in the present study is 25 cal/cm^3. Without attempting quantitative summations of enthalpies and free energies, it is nevertheless clear that the excess thermodynamic quantities and the Scatchard–Hildebrand heats and free energies of mixing are of the same orders of magnitude (but of opposite sign in the case of the heats).

Swelling and solution effects arising from the excess free energy of the glassy state have been or can be identified in other systems. For example, the swelling of polycarbonate by acetone[9] at various partial pressures is endothermal by about 14 cal/cm^3 of acetone above the T_g of the swollen polymer but is zero below the T_g. That the relationship between the degree of swelling and the partial pressure of acetone in this system changes abruptly at T_g (Figure 8), whatever the ambient temperature of the swelling experiment, is a direct consequence of this fact. This change is, moreover, a direct analog of the change in slope of the swelling envelope of Figure 4 at the point that $T_g = 25°$, since the abscissas in both cases reflect the free energy of mixing.

Excess enthalpies of the glass have in some cases been measured directly by solution calorimetry.[10] Another closely related observation is that the heats of solution of permanent gases in amorphous polymers are usually more endothermal above T_g than below.[11] The usual proffered explanation for this observation has been that below T_g solution of gas in glass involves the filling of preexisting holes, whereas above T_g the gas molecule has to "make" its own hole. The close relationship between these various solubility phenomena and rationalizations is evident.

(9) R. P. Kambour, F. E. Karasz, and J. H. Daane, *ibid.*, *Part A-2*, **4**, 327 (1966).
(10) J. Stoelting and F. H. Mueller, *Kolloid Z.-Z. Polym.*, **238**, 459 (1970).

Conclusions

On the basis of these observations and ideas and our general knowledge of crazing behavior, the prognosis is not good for finding a homogeneous glassy polymer of (a) high T_g and high resistance to crazing in the dry state and (b) immunity to reductions of crazing resistance by organic agents—even by those having very dissimilar solubility parameters from that of the polymer. Resistance to dry crazing is usually high only at temperatures far below T_g where the excess free energy of the glassy state is high, and thus the general driving force for absorption of limited amounts of plasticizing agents is great.

(11) P. Meares, *J. Amer. Chem. Soc.*, **76**, 3415 (1954); *Trans. Faraday Soc.*, **53**, 101 (1957).

Interpenetrating Polymer Networks of Poly(ethyl acrylate) and Poly(styrene-*co*-methyl methacrylate). I. Morphology *via* Electron Microscopy

Volker Huelck, D. A. Thomas, and L. H. Sperling*

Materials Research Center, Lehigh University, Bethlehem, Pennsylvania 18015.
Received February 2, 1972

ABSTRACT: Interpenetrating polymer networks (IPN's) have been synthesized by swelling a cross-linked rubbery polymer (I) with a second plastic monomer (II or III or II-*co*-III) plus initiator and cross-linking agent and polymerizing the second monomer *in situ*. IPN's have also been produced by inverting the order of preparation. According to the overall compositions, IPN's of elastomeric or leathery or plastic behavior have been obtained. Polymers employed were poly(ethyl acrylate) (I), polystyrene (II), and poly(methyl methacrylate) (III). Like most other types of polymer blends, IPN's exhibit a complex two-phase morphology. The electron micrographs show a characteristic cellular structure of about 1000-Å diameter simultaneously with a fine structure with phase domains of the order of 100 Å. In the midrange leathery materials the cell walls are composed of the second network polymer. The fine structure is observed most clearly within the cell walls, and probably originates through a second, later phase separation as polymerization continues beyond the initial cellular formation stage. Increasing compatibility of the two polymers is attained as methyl methacrylate mers replace styrene mers in the plastic component. This leads to the disappearance of the cellular envelopes but retention of the fine 100-Å domain structure. Inverting the sequence of preparation (swelling monomer I into network II or III) showed that the network synthesized first controls the morphology of the IPN's, comprizing the more continuous phase.

Interpenetrating polymer networks (IPN's) exhibit an intimate mixture of two polymeric networks which are superimposed within each other. IPN's are prepared by swelling a cross-linked polymer (I) with a second monomer solution (II or III or II-*co*-III) which contains an initiator and a cross-linking agent. An IPN results upon polymerizing the second monomer (or comonomer solution) *in situ*.[1-9]

In the previous papers on IPN's from this laboratory, the temperature and time dependencies of viscoelastic properties were presented.[1-3] The investigations showed that an incompatible IPN pair, poly(ethyl acrylate)–polystyrene

(1) L. H. Sperling and D. W. Friedman, *J. Polym. Sci., Part A-2*, **7**, 425 (1969).
(2) L. H. Sperling, D. W. Taylor, M. L. Kirkpatrick, H. F. George, and R. D. Bardman, *J. Appl. Polym. Sci.*, **14**, 73 (1970).
(3) L. H. Sperling, H. F. George, V. Huelck, and D. A. Thomas, *ibid.*, **14**, 2815 (1970).
(4) L. H. Sperling, V. Huelck, and D. A. Thomas, "Polymer Networks: Structural and Mechanical Properties," S. Newman and A. J. Chompff, Ed., Plenum Press, New York, N. Y., 1971.
(5) A. J. Curtius, M. J. Covitch, D. A. Thomas, and L. H. Sperling, *Polym. Eng. Sci.*, **12**, 101 (1972).
(6) J. R. Millar, *J. Chem. Soc.*, 1311 (1960).
(7) K. Shibayama and Y. Suzuki, *Kobunshi Kogaku*, **23**, 24 (1966).
(8) K. Shibayama and M. Kodama, *ibid.*, **24**, 1 (1967).
(9) K. Shibayama and M. Kodama, *ibid.*, **24**, 104 (1967).

TABLE I
COMPOSITION OF INVESTIGATED IPN'S

Series	Polymer	Wt % polymer 1	2	3	4
E	PEAB	74.4	75.9	75.5	72.2
	P(S-*co*-MMA)	25.6–0	15.7–8.4	9.9–14.6	0–27.8
L	PEAB	48.8	51.2	48.4	47.1
	P(S-*co*-MMA)	51.2–0	23.4–25.4	13.6–38.0	0–52.9
P	PEAB	23.9	24.7	25.4	23.3
	P(S-*co*-MMA)	76.1–0	40.9–34.4	24.9–49.7	0–76.7
I	PS	24.6	50.7	71.4	0
	PMMA	0	0	0	77.5
	PEAB	75.4	49.3	28.6	22.5

(PEA–PS), exhibits two distinct glass transitions, and that a semicompatible IPN pair, poly(ethyl acrylate)–poly(methyl methacrylate) (PEA–PMMA), exhibits one single broadened glass transition covering the region between the transitions of the two homopolymers. Preliminary electron micrographs of two IPN's[4,5] revealed a complex cellular structure with supporting evidence for interpenetration between the two networks.

In the present study, fine structures of three IPN series of different compositions of PEA/P(S-*co*-MMA) were investigated: 75/25, 50/50, and 25/75. Also an inverse series was prepared, wherein the plastic component was polymerized first. Within each series it was of interest to explore the change in compatibility *via* electron microscopy as S-mers in the plastic network are gradually replaced by MMA-mers.

The second paper in this series will deal with the dynamic mechanical behavior and also the ultimate properties of these IPN's. While electron microscopy shows the size and shape of the phase domains, dynamic mechanical spectroscopy, especially the loss modulus, E'', as a function of temperature, reveals the extent of molecular mixing.

Materials and Synthesis

All IPN's were synthesized by photopolymerization techniques previously described.[1,2] In brief, a monomer containing dissolved benzoin as initiator and tetraethylene glycol dimethacrylate (TEGDM) as cross-linking agent was polymerized by exposure to ultraviolet sunlamps. The ratio throughout was 0.5 ml of TEGDM and 0.3 g of benzoin per 100 ml of monomer, which was ethyl acrylate, methyl methacrylate, or styrene. After vacuum drying the homopolymeric network to constant weight to remove the unreacted monomer (usually less than 2% weight loss), network I was swollen with the second monomer solution. The duration of imbibing depended on the desired overall composition. The second monomer was then polymerized *in situ*, after uniformity of composition had been attained through diffusion. This was followed by a second drying step where again only 1–2% weight loss was observed. Several samples were also exposed to swelling and extraction studies. As expected, the materials swelled, but did not dissolve, confirming the network characteristics. Only 1–2% extractables by weight were observed. No study was made of the composition of the volatiles or extracted material.

Four series of IPN's have been polymerized, the compositions of which are given in Table I. The underlined polymer has been polymerized first. This was always the elastomeric PEA (normal IPN's), except for series I (inverse series), where the plastic homopolymer PS or PMMA was polymerized first. The B in PEAB indicates that the PEA contains a trace of butadiene as a comonomer, as discussed below. The letters E, L, P, and I denote eleastomeric, leathery, plastic and inverse series, respectively. In compositions containing both S- and MMA-mers, a random copolymer is formed with the indicated composition. The actual compositions employed in this investigation can be portrayed with the aid of a pseudoternary phase diagram, as shown in Figure 1 for the normal IPN's. Only the border compositions (no random copolymers) were investigated in the inverse materials. The normal and inverse nomenclature is arbitrary, and depended only on which was synthesized earlier. In all cases a small quantity of butadiene (*ca.* 1%) was added to the EA as a comonomer before polymerization. The purpose of incorporating the butadiene was to make available carbon–carbon double bond sites for osmium tetroxide staining of electron microscopy specimens.

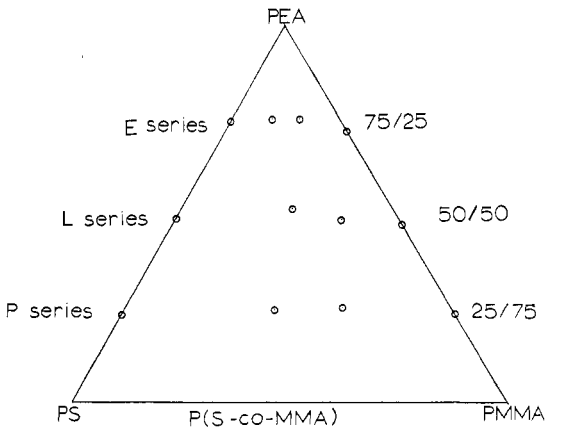

Figure 1. Ternary composition diagram showing materials examined in this paper. Note that styrene and methyl methacylate compositions are random copolymers of the two.

Series L, which contains approximately 50 wt % PEAB, provides leathery materials, while series E, which contains *ca.* 75 wt % PEAB, yields self-reinforcing elastomeric materials. Series P contains only approximately 25 wt % PEAB and exhibits properties of toughened plastics. In an IPN the component polymerized first is always strained due to the diffusional swelling forces of the second monomer solution. Therefore, it was of particular interest to prepare an inverse series of IPN's (series I) where the plastic component was polymerized first. Since the compositions of this series are almost identical with some of the border compositions (containing only one plastic-forming mer) of the L, E, and P series, they may be effectively compared with those. The following samples match in overall composition (see Table I): I1/E1, I2/L1, I3/P1, I4/P4.

The reasons underlying the selection of the three monomers involved should be mentioned. PEA and PMMA are chemically isomeric, and hence expected to be much more compatible toward each other than the PEA–PS pairs, which are known to be incompatible. On the other hand, PMMA and PS have glass–rubber transitions of 105 and 100°, respectively. As a result, their random copolymers will have essentially the same glass-transition temperatures (iso T_g) as the plastic homopolymers. This last will simplify the interpretation of the mechanical results to be presented in part II.[10]

It is important to consider possible grafting between the two networks. There are two major sites for grafting in the

(10) V. Huelck, D. A. Thomas, and L. H. Sperling, *Macromolecules*, 5, 348 (1972).

materials employed: (1) the α-hydrogens in the TEGDM cross-linking agent[11] and (2) the tertiary hydrogens in the PEA. In addition, the residual double bonds in the PEAB are vulnerable. Preliminary calculations indicate that intramolecular cross-links are considerably more numerous than intermolecular grafts. Thus for certain simple properties the networks may be considered chemically independent. For other properties, such as impact strength, even limited amounts of grafting may be crucial. Further experiments are planned to test these variables.

The exact compositions of the IPN's as given in Table I were determined in the following ways. When the samples were made up only from two homopolymers, the weight difference before and after the second polymerization step provided the necessary information. This was the case with all border compositions of the series E, L, and P, as with all IPN's of series I. The remaining samples contained a random copolymer of P(S-*co*-MMA) as the plastic phase. Since the rate of diffusion of MMA into PEA was smaller than for S, the MMA fraction of the plastic IPN phase was smaller than its part in the monomer solution, *i.e.*, only the overall amounts of the elastomeric and the plastic phases could be determined *via* weight difference. These samples were analyzed for C and H content by Robertson Laboratory, Florham Park, N. J., which allowed the calculation of the actual S/MMA ratio. For comparison, the samples containing two homopolymers (border compositions) were also analyzed in this way. In all cases the compositions calculated were in exact agreement with the ones obtained *via* weight difference. In all calculations the traces of butadienemer in the elastomeric phase were disregarded.

Electron Microscopy

The sample preparation technique used was based on Kato's famous OsO_4 staining technique[12a] and on Matsuo's two-step sectioning method.[12b] Three pieces per sheet of a polymerized IPN of approximately $0.3 \times 0.5 \times 10\,mm^3$ were exposed to OsO_4 vapor at room temperature for a period of 2 weeks in order to selectively stain the butadiene-mer portion of the PEAB phase. Sections of these stained pieces of about $0.1 \times 0.1 \times 2\ mm^3$ were imbedded in an epoxy resin, such that the long dimension of the section was perpendicular to the cutting direction of the microtome. A Porter-Blum MT-2 ultramicrotome equipped with a diamond knife was used for ultrathin sectioning at room temperature. A thickness of approximately 400 Å yielded satisfactory results. Transmission electron micrographs were taken by direct observation of the ultrathin sections employing an RCA EMU-3G electron microscope.

Results

In general, all electron micrographs revealed a complex structure, including cellular formation and a fine structure within the cell walls. The osmium tetroxide stained PEAB domains appear black or dark grey in the following, while the unstained plastic regions are whitish or light grey.

(1) Leathery Series. Because the leathery 50/50 compositions exhibited the greatest heterogeneity, this series was selected for the most intensive investigation. Figures 2–5 show photomicrographs of series L (L1, L2, L3, and L4).

(11) Dr. W. White, NL Industries, Inc., Hightstown, N. J., private communication.

(12) (a) K. Kato, *J. Polym. Sci., Part B*, 4, 35 (1966); *Polym. Eng. Sci.*, 7, 38 (1967); (b) M. Matsuo, T. K. Kwei, D. Klempner, and H. L. Frisch, *ibid.*, **10**, 327 (1970).

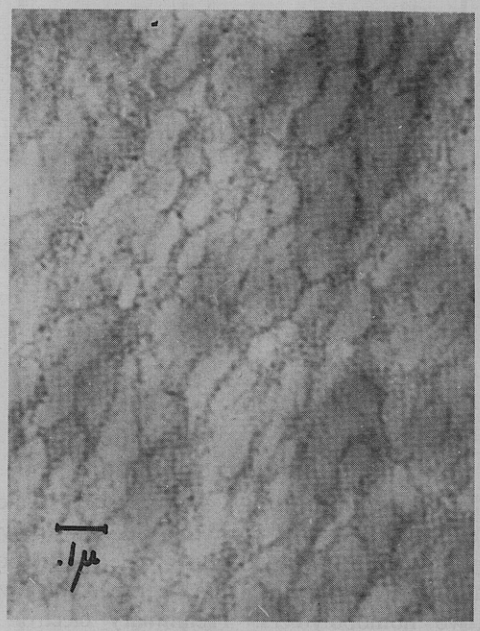

Figure 2. Electron micrograph of IPN L1: 48.8 PEAB/51.2 PS. Note appearance of a cellular structure and a fine structure within the cell walls.

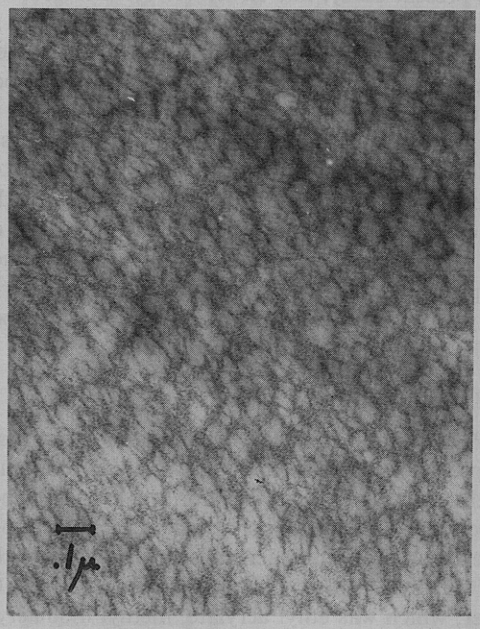

Figure 3. Electron micrograph of IPN L2: 51.2 PEAB/P (23.4 S-*co*-25.4 MMA). The smaller cell structure than shown in Figure 1 may arise because initial phase separation took place later in the second polymerization step.

Sample L1 exhibits a complex cellular morphology (Figure 2). The cell walls are largely PEAB, the inner cell domains being mainly PS. A fine structure is observed mainly within the cell walls but also—however, weaker and not as frequently—inside the cells. In the first case PS domains are pervading the PEAB walls, whereas in the latter PEAB particles are pervading the cells. The sizes of the cells are approximately 1000 Å. The PEAB and the PS microstructures are of the order of 100 Å. Although the cells are irregularly shaped, they exhibit a certain orientation which coincides with the radiation direction of the polymerization. Large darker areas, often arranged in forms of streaks, are not a morphological feature. They result from the microtoming process and coincide with the cutting direction.

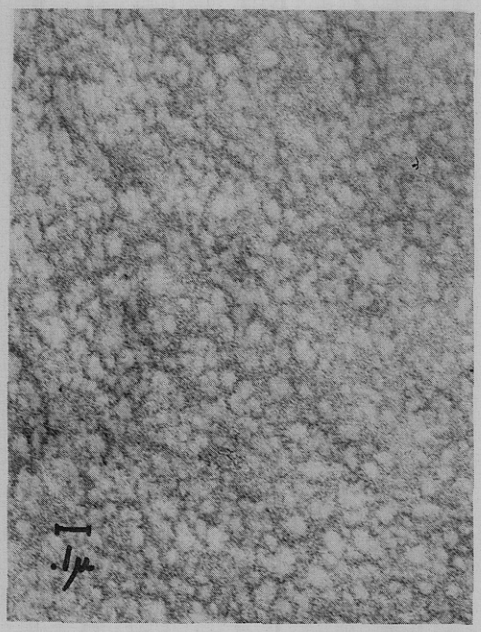

Figure 4. Electron micrograph of IPN L3: 48.4 PEAB/P (13.6 S-*co*-38.0 MMA). The cell structure is much less well defined, giving way to the fine structure.

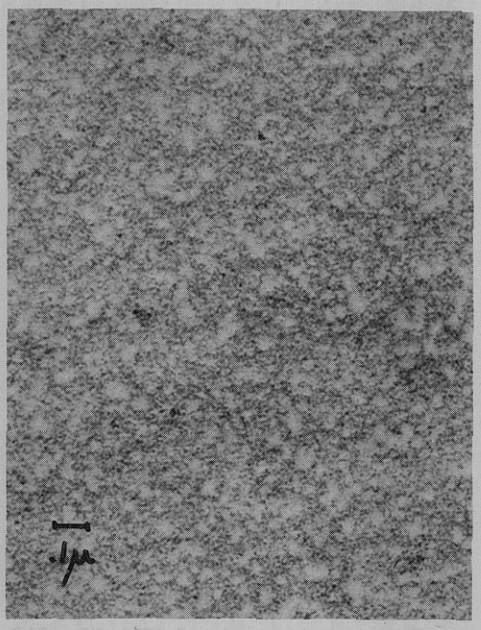

Figure 5. Electron micrograph of IPN L4: 47.1 PEAB/52.9 PMMA. This isomeric IPN does not exhibit a cellular structure in the sense of Figures 1–3, but some division of the phases is retained. PEAB and PMMA may be regarded as being semicompatible.

Figures 3 and 4 show electron micrographs for IPN compositions of L2 and L3, respectively. The cell walls become less distinct as S-mers are gradually replaced by MMA-mers. Furthermore, the areas of fine dispersion increase. One notices a decrease in the fine structure domain size to below 500 Å as well as a decrease in the cell size down to about 100–600 Å. It seems as though the plastic-rich cells are increasingly pervaded by PEAB starting from the walls. Sample L4 in Figure 5 shows a more compatible structure than the previous ones. The cell walls are completely disintegrated, although PMMA phase domains remain without marked boundaries. The latter are between 300 and 500 Å in diameter, whereas the distinct fine structure PEAB domains are below 100 Å in diameter.

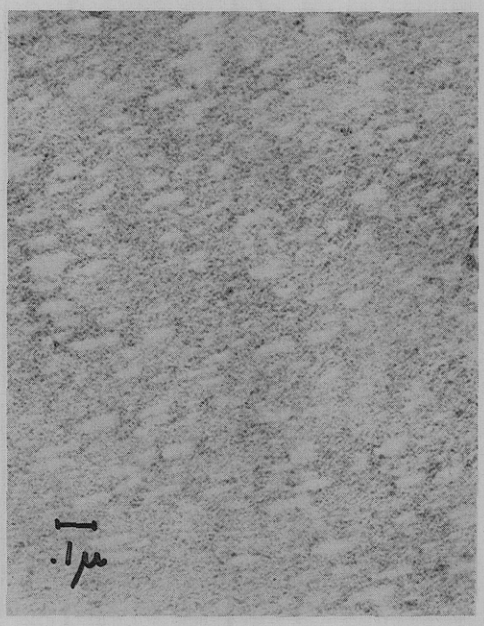

Figure 6. Electron micrograph of IPN E1: 74.4 PEAB/25.6 PS. This self-reinforcing elastomer has a morphology reminiscent of the block-copolymer thermoplastic elastomers.

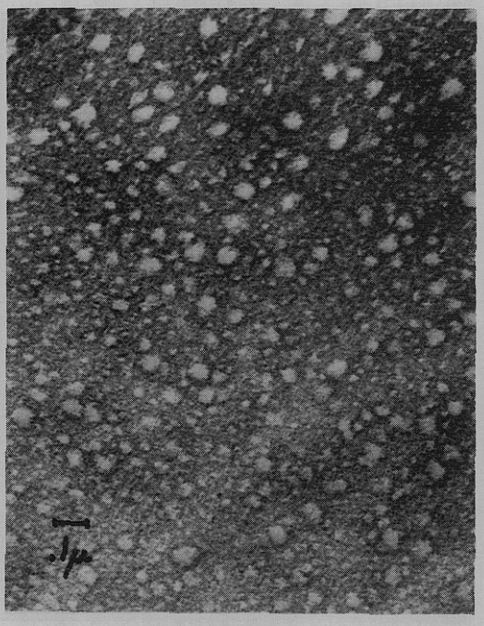

Figure 7. Electron micrograph of IPN E2: 75.9 PEAB/P (15.7 S-*co*-8.4 MMA).

(2) Elastomeric Series. The morphologies of the elastomeric series are given in Figures 6–9. Figure 6 shows the microstructure of sample E1. The basic matrix shows what appear to be two continuous phases. The larger oriented white areas are part of the PS matrix which does not contain any rubbery material. They vary considerably in size, the longer dimension being between 800 and 1500 Å. The PEAB particles are again approximately 100 Å in diameter.

Figure 7 (sample E2) reveals the influence of MMA in the plastic phase. The pure plastic areas are more numerous than in Figure 6 and cover a wider region in domain size (from 200 to 750 Å). Sample E3, Figure 8, shows a structure similar to that of sample E2. However, the number of pure

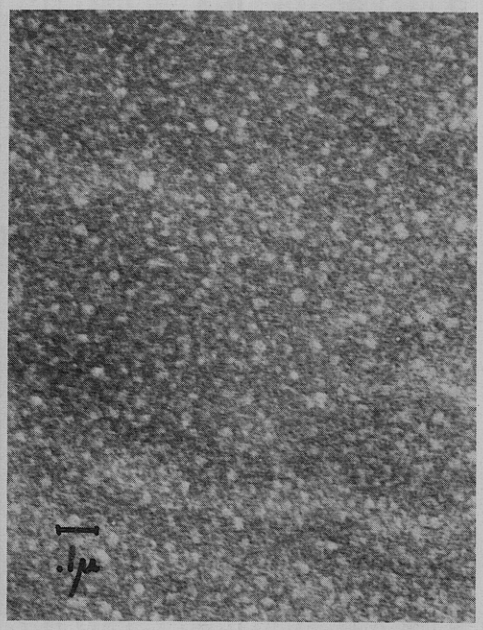

Figure 8. Electron micrograph of IPN E3: 75.5 PEAB/P (9.5 S-*co*-14.6 MMA). The cellular structure is smaller than found in Figure 6.

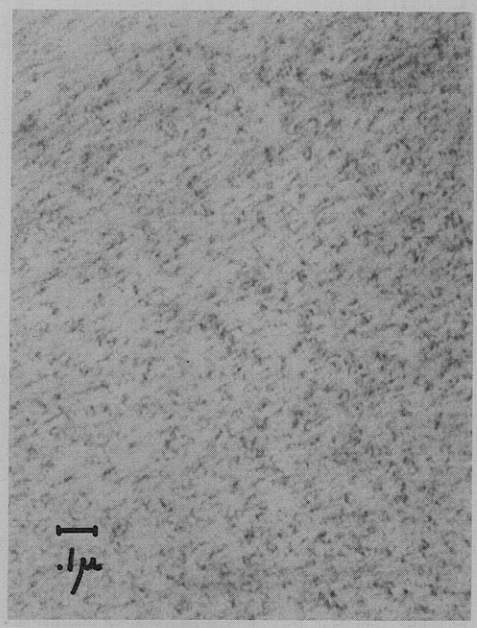

Figure 10. Electron micrograph of IPN P1: 23.9 PEAB/76.1 PS. This material is the counterpart of the impact-resistant graft-type polymer blends.

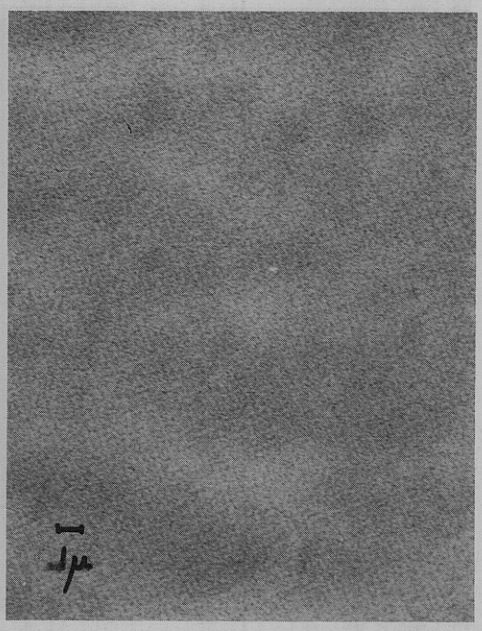

Figure 9. Electron micrograph of IPN E4: 72.2 PEAB/27.8 PMMA. No cellular structure exists for this composition, only the fine structure is present. As explained in the text, the fine structure domain dimensions are about the same size as the end-to-end distance of the polymer segments between cross-link sites.

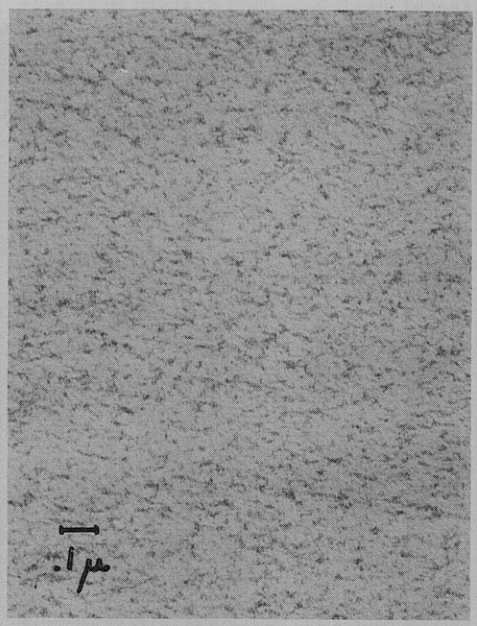

Figure 11. Electron micrograph of IPN P2: 24.7 PEAB/P (40.9 S-*co*-34.4 MMA).

plastic domains has increased again, whereas the average size is somewhat smaller. The final figure in this series, Figure 9, corresponds to sample E4, which does not contain any S-mers. It shows a very fine dispersion of PEAB particles in PMMA, and *vice versa*. No remnants of the cellular structure are observed; this sample is composed of fine structures only.

(3) Plastic Series. The morphology of the plastic IPN series is shown in Figures 10–13. Throughout this series, both phases seem to exhibit some degree of phase continuity, but the PEA component appears the more continuous. As long as the samples contain a certain amount of S (samples P1, P2, and P3), traces of a cellular structure are revealed. However, the interconnected spheroids of PEAB do not form long enough particulate chains in order to surround the plastic cell core completely; *i.e.*, the vast majority of the cells are not closed. The differences between samples P1, P2, P3, and P4 as observed on the electron micrographs are small. The sizes of the cellular traces are approximately 1000 Å. Sample P4 in Figure 13 shows small remainders of a cellular structure with weakly marked walls.

(4) Inverse IPN's. Sample I1 (Figure 14) reveals clear indications of a cellular structure. PS or a PS-rich phase is the more continuous matrix which contains PEAB-rich cells.

Figure 15 shows the morphology of sample I2. Like its countercomposition (sample L1 in Figure 2), it exhibits a complex but approximately inverse cellular structure, a PS-

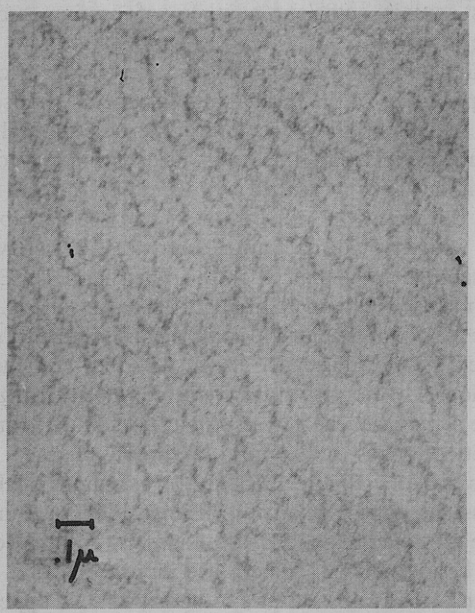

Figure 12. Electron micrograph of IPN P3: 25.4 PEAB/P (24.9 S-*co*-49.7 MMA). The cell boundaries are rather poorly defined.

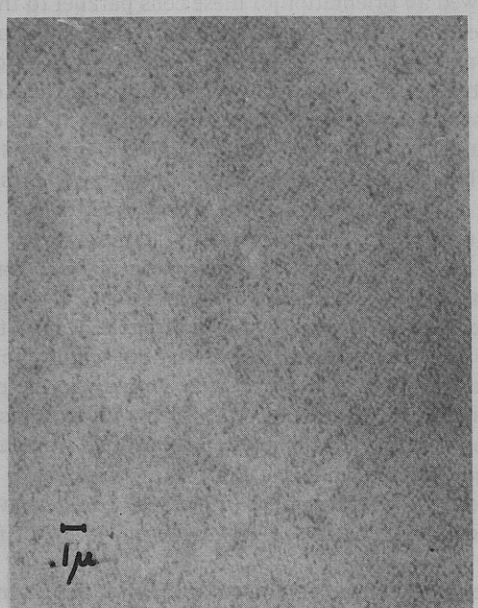

Figure 13. Electron micrograph of IPN P4: 23.2 PEAB/76.7 PMMA. As in Figure 8, no cellular structure was found.

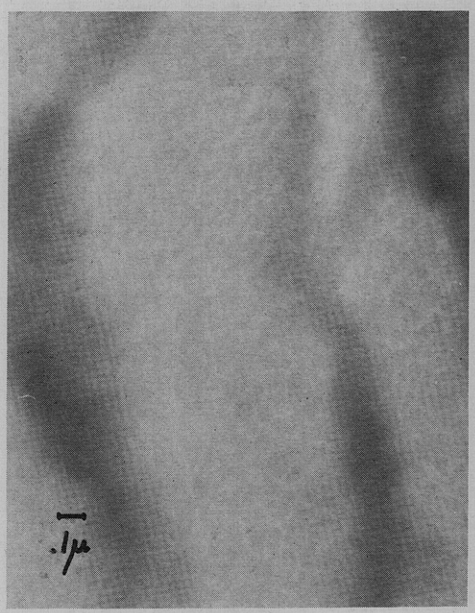

Figure 14. Electron micrograph of IPN I1: 24.6 PS/75.4 PEAB.

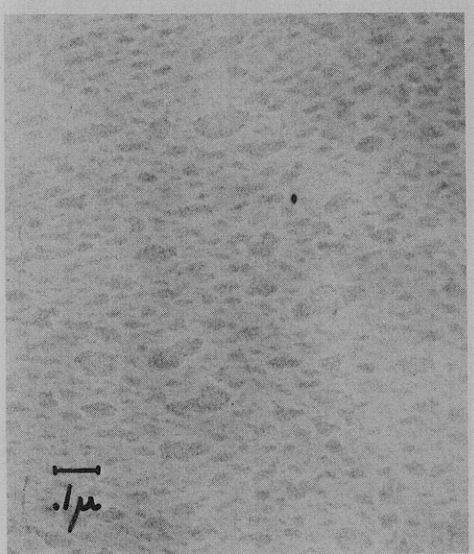

Figure 15. Electron micrograph of IPN I2: 50.7 PS/49.3 PEAB. This structure is the inverse of that shown in Figure 1. The first component forms the matrix material and exhibits greater continuity than the second component.

rich matrix containing PEAB-rich cellular inclusions. The cellular domains cover a wide size range; the longer dimension of the stretched cells are between 400 and 2000 Å and the smaller ones are between 150 and 1000 Å. The fine structure domains are somewhat smaller than 100 Å.

The morphology for the inverse plastic IPN of sample I3 is shown in Figure 16. PEAB particles or agglomerates of a few particles up to 150 Å are regularly dispersed in the PS matrix. In many cases they appear to have started to form loosely connected cell boundaries which are incomplete and never closed. The micrograph of the plastic inverse IPN I4 (Figure 17) exhibits a uniform fine structure which is very similar to its normal countercomposition P4 (Figure 13). PMMA probably forms the more continuous phase with both samples; however, this is difficult to determine. The electron micrographs show finely dispersed particles which are clearly below 100 Å in diameter. Sample I4 shows, besides the interpenetrating structure, randomly dispersed dark spots *ca.* 150 Å in diameter, which might be agglomerates of PEAB particles.

Discussion

(1) OsO_4 Staining. Kaempf and Schuster[13] have shown that an exact representation of the stained phase depends on an adequate OsO_4 fixation, *i.e.*, the proper exposure time. They showed that flattening of spherical rubber particles was caused by too little fixation, while too much fixation resulted in swelling of the particles. In both cases excessive particle diameters were measured.

(13) G. Kaempf and H. Schuster, *Angew. Makromol. Chem.*, **14**, 111 (1970).

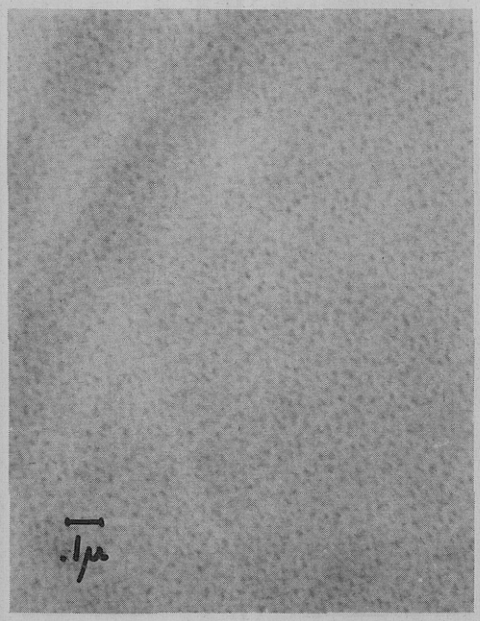

Figure 16. Electron micrograph of IPN I3: 91.4 PS/28.6 PEAB.

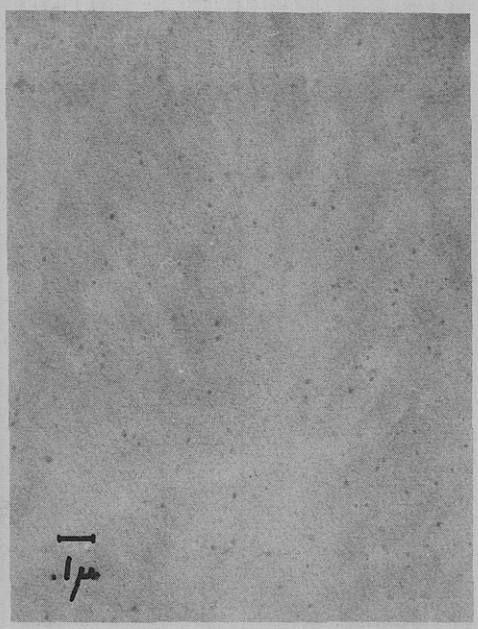

Figure 17. Electron micrograph of IPN I4: 77.5 PMMA/22.5 PEAB.

The amount of butadiene employed results in a random copolymer of EA and B with an approximate concentration of one butadiene mer per 50 or 100 EA-mers. Assuming one osmium tetroxide unit per two double bonds, a stained spherical particle of 100-Å diameter contains approximately ten OsO_4 molecules. The photographic contrast, therefore, is not as good as it would be with an unsaturated rubber phase such as polybutadiene, and the stained portions of the IPN electron micrographs do not exactly represent the complete domain area of the rubber phase even under the assumption of total fixation of the incorporated butadiene-mers. The dark stained PEAB domains are therefore expected to be somewhat smaller than the actual PEAB particles, although the measurements are considered to be of the right magnitude. However, the dimensions of the arrays of stained PEAB particles (*e.g.*, interconnected spheroids in the cellular formations) probably are indicated with fairly good accuracy. Owing to the larger size of the cellular structures, these gross domains contain sufficient numbers of osmium atoms for accurate portrayal.

(2) Micromorphological Features. Let us first compare the morphologies of the normal and inverse materials. Considering the 50/50 PEA/PS compositions, the normal sample L1 (Figure 2) yields big differences when compared to Figure 15, in spite of the same overall composition. Certain features seem to be black–white inversions. The cellular content is PS rich with the normal sample and PEAB rich with the inverse sample. The matrix, on the other hand, is PEAB rich for the normal IPN and PS rich for the inverse IPN. However, the matrix of the normal sample consists mainly of interconnected PEAB spheroids. As a result of comparing the morphologies of normal and inverse compositions, generally it can be stated that the network synthesized first forms either the continuous phase or the more continuous phase.

With sample I2 (Figure 15), the border regions of the cellular inclusions appear relatively distinct. This is surprising, since the matrix contains PEAB besides PS and the cells contain PS besides PEAB. There are indications that the PS-rich matrix is not of constant composition. It appears that the PS concentration of the matrix is particularly high in the vicinity of the walls, which would cause the rather clear distinction between the cell walls and matrix.

All the IPN samples exhibiting a complex cellular structure showed an orientation of these cells parallel to the radiation direction. The ratio of the long dimension over the broad one very seldom exceeded a value of 2, which leads one to believe that the cells might approximately describe an ellipsoidal envelope in three dimensions. The electron micrographs show a cross section through the plastic ellipsoids. These cross sections vary considerably in size, depending on the thickness of the microtomed slices and the position of the domain equator relative to the section.

Since the PS domains are transparent to electrons at a thickness of 500 Å, the stained interconnected PEAB spheroids of the cellular envelope are still observable even if they are spatially above or below a PS portion but within the section under examination. An alternate hypothesis to the presence of fine structure within the cells relates to the presence of entrapped chains of the first component, which segregate upon continued polymerization. Both the see-through artifact and the entrapped chain mechanisms may be operative, however, and it remains for further experiments to clarify this point.

It should be clearly understood from the "sandwich" polymerization method that all electron micrographs examined represent the structure of a plane which was parallel to the direction of radiation. Thus, the question arises as to whether the morphology and properties in a plane normal to the radiation would differ. Extreme examples of vast morphological differences in two normal directions have been demonstrated by Matsuo and coworkers[14–16] and have been discussed by Molau,[17] where, *e.g.*, with block copolymers cylindrical rods appear like spheroids in a normal plane. While the above electron micrographs are not conclusive, the structures will behave nearly isotropically provided the differences in the long and broad dimensions of the cells are less than a factor of approximately 2.

(14) M. Matsuo, *Jap. Plastics*, 2, 6 (July, 1968).
(15) M. Matsuo, C. Nozaki, and U. Tyo, *Polym. Eng. Sci.*, 9, 197 (1969).
(16) M. Matsuo and S. Sagaye, "Colloidal and Morphological Behavior of Block and Graft Copolymers," G. E. Molau, Ed., Plenum Press, New York, N. Y., 1971.
(17) G. E. Molau in "Block Polymers," S. L. Aggarwal, Ed., Plenum Press, New York, N. Y., 1970.

Although electron micrographs of numerous two-phase polymeric systems have been published,[16-20] there are only very few examples[15,16] known where the heterogeneity between the two phases is found at a 100-Å level or below. This indicates that the technique for preparing IPN's of PEA, PS, and PMMA provides extremely fine structures and thus emphasizes the special position of IPN's within polyblends.

The effect of replacing S-mers by MMA-mers on phase separation requires further examination. The cellular structures definitely decrease in size and become less distinct with increasing MMA-mer content. In a few cases, notably in Figures 9 and 13, the cellular structure appears entirely absent. While the exact relationship between cell size and compatibility remains unknown, probably the free energy of phase separation is important. Noting the isomeric relationship between MMA- and EA-mers and the increased compatibility of PEA–PMMA systems over PEA–PS systems, the evidence suggests that primary phase separation takes place later in the second-stage polymerization the greater the MMA/S ration. The fine structure always appears, and indeed assumes the dominant role in the morphology of semicompatible materials. While it appears possible that the fine structures are actually nascent nucleated cellular structures, they are more likely a result of a secondary phase separation, as discussed below.

(3) Optical Properties. A few comments are in order concerning the clarity of the IPN's. The PEA–PS compositions are quite opalescent and obviously phase separated to the naked eye. As MMA-mers replace S-mers, the material becomes progressively clearer, having a clarity approaching PMMA homopolymer when S-mers are entirely absent. Two possible causes should be considered. As the domains become progressively smaller, the scattering of light is quantitively decreased. Also, as MMA replaces S-mers, the refractive indices of the two components become progressively closer,[21,22] since PEA and PMMA are chemically isomeric. In this case clarity emphatically does not denote compatibility, although this is often true.

(4) The Interpenetration Problem. The electron micrographs as such cannot prove interpenetration. Among other methods, a Maxwell's demon could prove such things. However, it is instructive to critically review the evidence concerning interpenetration and continuity of the phases and components at this point.

(a) Certainly the two-phased nature of IPN's indicates that we are principally concerned with interpenetration on a supermolecular scale, rather than on a true molecular scale. Evidence for the existence of trapped molecules, another form of interpenetration, is given by the unexpected inward shifting of the two glass transitions, as will be discussed in part II of this series.[10]

(b) The first network as a component is clearly continuous on a macroscopic scale. This is obvious from both a simple inspection of the sample during IPN synthesis and electron microscopy observations that the first network always forms the matrix.

(c) Although the bulk of the second network appears to lie within the cells, the 100-Å fine structure within the matrix is a clue to the continuity of the second network. A proposed model of the fine structure pervading the cell walls and connecting the cell contents is shown in Figure 18. This model is reminiscent of the old fringed micelle model of polymer crystallinity.

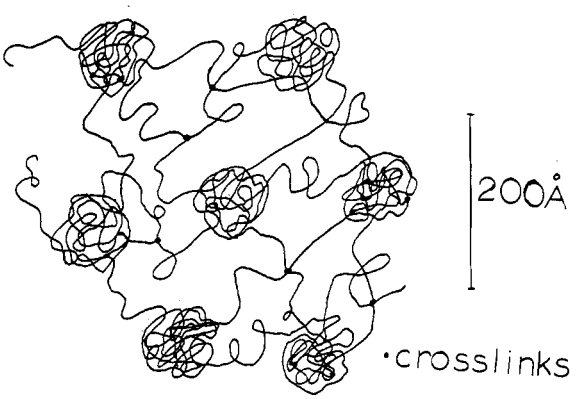

Figure 18. Model of the interpenetration mode through the cell wall structures. Note that the fine structures have dimensions smaller than the end-to-end distances of most macromolecules.

(d) The fine structure exhibits domain dimensions of the order of 100 Å or less. This is the same order of magnitude as the expected end-to-end distances of a polymer segment between cross-link junctures (*ca.* 200 mers) and much smaller than the end-to-end distance of the primary chains. If we accept a model similar to Figure 18, the phases need not be continuous, but the components must be if the second polymer formed a reasonable network. It should be pointed out that the domains observed here are much smaller than the partially interpenetrating elastomeric networks of Frisch.[12]

(e) In some electron micrographs, notably Figures 5, 9, and 13, no cellular structure remains. It becomes difficult to determine which, if either, of the phases predominates. As in George Orwell's "Animal Farm," it may be more correct to state that "All animals are equal, but some are more equal than others."

Conclusions

IPN's exhibit a complex cellular structure. The electron micrographs reveal a characteristic cellular morphology of about 1000 Å simultaneously with a fine structure with phase domains of the order of 100 Å. The cellular envelopes gradually disappear as MMA-mers replace S-mers in the plastic component. While the PEA–PS polymer pair is incompatible, it may be more accurate to describe the PEA–PMMA pair as semicompatible. Inverting the sequence of preparation showed that the network synthesized first controls the morphology of the IPN's by forming the more continuous matrix, but did not result in an exact inversion of morphology.

A comparison of the phase separation modes of graft-type polymer blends with IPN's leads to a prediction of a fine structure within the cell walls of the former. Its nature however, must be different, because cross-linking is absent. We also examined the continuity of the two components and conclude that circumstantial evidence supports the concept of two continuous components on a macroscopic scale for all materials examined. Two continuous phases appear to exist in some samples, especially among the semicompatible systems.

Acknowledgments. The authors wish to thank the National Science Foundation for financial support through Grant No. GK-13355. We also wish to thank Dr. M. Matsuo of the Bell Telephone Laboratories and the Japanese Geon Co. for his many helpful discussions.

(18) K. Kato, *Jap. Plastics*, 2, 6 (April, 1968).
(19) E. R. Wagner and L. M. Robeson, *Rubber Chem. Technol.*, 43, 1129 (1970).
(20) G. E. Molau, *J. Polym. Sci., Part A*, 3, 1267 (1965).
(21) S. L. Rosen, *Polym. Eng. Sci.*, 7, 115 (1967).
(22) B. D. Gesner, *J. Appl. Polym. Sci.*, 11, 2499 (1967).